

Affordable Spectral Measurements of Translucent Materials: Supplemental Document

TOMÁŠ ISER, Charles University, Czech Republic

TOBIAS RITTIG, Charles University, Czech Republic

EMILIE NOGUÉ, Imperial College London, United Kingdom

THOMAS KLAUS NINDEL, Charles University, Czech Republic and Berufsakademie Sachsen, Germany

ALEXANDER WILKIE, Charles University, Czech Republic

This document supplements the following main article:

Tomáš Iser, Tobias Rittig, Emilie Nogué, Thomas Klaus Nindel, and Alexander Wilkie. 2022. Affordable Spectral Measurements of Translucent Materials. *ACM Trans. Graph.* 41, 6, Article 199 (December 2022), 13 pages. <https://doi.org/10.1145/3550454.3555499>

1 INTRODUCTION

This document supplements the main article about affordable spectral measurements of translucent materials. Its intention is to analyze major problems that many existing measurement methods suffer from (Sec. 2), and provide a list of components that we used to build a prototype of our method (Sec. 3). We also attached an STL file that contains the geometry of our custom-made background holder, and is ready to be 3D printed with standard FDM printers.

2 ANALYSIS

We analyze two major problems that many existing approaches suffer from. We start by discussing the issues associated with non-spectral measurements based on RGB acquisitions (Sec. 2.1). And we follow by introducing the similarity relations and why they make it difficult to measure material’s phase function in a simple measurement geometry (Sec. 2.2).

2.1 Issues with RGB acquisition of material parameters

In the main article, we discussed several methods that measure optical properties in an RGB color space. They are convenient as they can be performed with a standard color camera. However, relying on RGB data instead of spectral measurements can lead to mispredictions due to several reasons that we discuss below. While some of them, like metamerism or energy conservation, are rather well known and also impact surface reflectance, transmission color shifting is specifically problematic for translucent materials.

Transmission color shifts. Light transmittance through a translucent medium has an exponential dependency on the distance ℓ traveled through the material, as defined in Beer’s law:

$$T(\ell, \lambda) = \exp(-\ell \cdot \sigma_t(\lambda)), \quad (1)$$

Authors’ addresses: Tomáš Iser, tomas@cgg.mff.cuni.cz, Charles University, Faculty of Mathematics and Physics, Malostranské nám. 25, Prague, 118 00, Czech Republic; Tobias Rittig, tobias@cgg.mff.cuni.cz, Charles University, Faculty of Mathematics and Physics, Malostranské nám. 25, Prague, 118 00, Czech Republic; Emilie Nogué, e.nogue@imperial.ac.uk, Imperial College London, Exhibition Rd, South Kensington, London, SW7 2BX, United Kingdom; Thomas Klaus Nindel, thomas@cgg.mff.cuni.cz, Charles University, Faculty of Mathematics and Physics, Malostranské nám. 25, Prague, 118 00, Czech Republic and Berufsakademie Sachsen, Hans-Grundig-Strasse 25, Dresden, 01307, Germany; Alexander Wilkie, wilkie@cgg.mff.cuni.cz, Charles University, Faculty of Mathematics and Physics, Malostranské nám. 25, Prague, 118 00, Czech Republic.

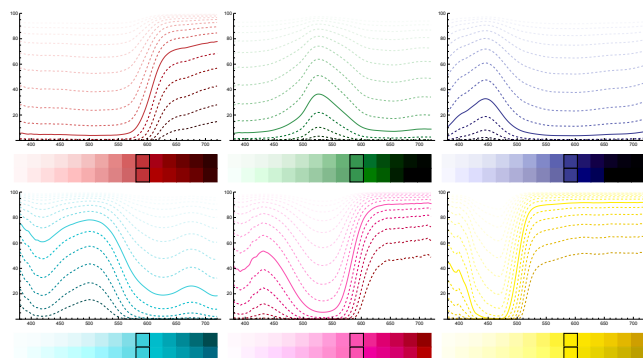


Fig. 1. A comparison of applying Beer’s law, Eq. (1), to spectral extinction coefficients $\sigma_t(\lambda)$, versus applying it to RGB triplets $(\sigma_t^R, \sigma_t^G, \sigma_t^B)$. The solid lines in the plots show original spectral data for various colored materials. The dotted lines show the resulting spectral shapes for shorter (above the solid line) and longer (below) transmission distances. The colored squares show the resulting transmission colors based on spectral data (top), and on RGB data (bottom). The outlined squares show a perfect match, because the RGB extinction coefficients were fitted to them. The colors of all other squares, however, diverge from the correct spectral results.

where $\sigma_t(\lambda)$ is the *extinction coefficient* of the medium. Because this non-linear equation is affecting each wavelength independently, it causes color shifting as light propagates further through the medium with increasing ℓ – an effect that we call *spectral sharpening*. In Fig. 1, we compare color predictions based on Eq. (1) applied to RGB extinction coefficients, in contrast to actual spectral $\sigma_t(\lambda)$. The results are visualized with their corresponding colored squares. The initial color is marked with a black outline, and the colors on the left and right correspond to shorter and longer distances ℓ , respectively. We can clearly see that the RGB and spectral predictions differ. Note that this problem is independent on an illuminant.

Metamerism. Appearance under *different illuminants* is a separate problem. One of the main properties of RGB color values is that there exists an infinite number of spectra $I(\lambda)$ corresponding to the same RGB triplet. This phenomenon is called *metamerism* [Wyszecki and Stiles 1982]. One of the consequences is that two different materials with reflectances $R_1 \neq R_2$, or transmittances $T_1 \neq T_2$, can both result in an identical *rgb*-triplet under a given illuminant with irradiance $L_1(\lambda)$, but they can have mismatched appearance under a different illuminant $L_2 \neq L_1$. For example, in the red channel with

a spectral sensitivity $\bar{r}(\lambda)$, it can hold:

$$\int \bar{r}(\lambda)R_1(\lambda)L_1(\lambda)d\lambda = \int \bar{r}(\lambda)R_2(\lambda)L_1(\lambda)d\lambda, \text{ although} \quad (2)$$

$$\int \bar{r}(\lambda)R_1(\lambda)L_2(\lambda)d\lambda \neq \int \bar{r}(\lambda)R_2(\lambda)L_2(\lambda)d\lambda. \quad (3)$$

This shows that appearance under different illuminants cannot be reliably predicted in purely RGB workflows, and instead requires spectral data. Reversing RGB triplets into spectra is an ill-posed problem called *spectral upsampling*, which is a research topic of its own [Jakob and Hanika 2019; Jendersie 2021; Jung et al. 2019].

Energy conservation. Every RGB color space can represent a particular subset (gamut) of all possible colors. One of the issues with using common color spaces for measurement purposes is that colors that are out of its gamut need to be represented with negative values or values above unity, which are not physically meaningful and break energy conservation. Gamut mapping these values, or just simply clipping them to a permissible range, introduces color shifts and therefore inaccuracies in the prediction.

2.2 Phase function and similarity relations

The similarity relations [Wyman et al. 1989; Zhao et al. 2014] describe ambiguities between materials of different bulk optical properties. In general, they say that under specific conditions, objects of different optical properties appear identical. This poses a problem for measurement methods, because if we observe identical appearance, we cannot distinguish the properties.

First-order similarity relations. Assuming a material with the Henyey-Greenstein phase function with a scattering anisotropy g , and absorption and scattering coefficients σ_a, σ_s , the following holds true. Under certain illumination and geometry conditions that result in a linearly anisotropic radiance field, which happens for example under a uniform diffuse light, there exist infinitely many combinations of material parameters (σ_a, σ_s, g) that yield identical appearance. In particular, two different materials will appear identical if they satisfy:

$$\sigma_a^* = \sigma_a, \quad \sigma_s^*(1 - g^*) = \sigma_s(1 - g), \quad (4)$$

where (σ_a, σ_s, g) and $(\sigma_a^*, \sigma_s^*, g^*)$ are the parameters of the first and second material, respectively.

This has two interesting consequences. First, on the positive side, this means that there are circumstances under which one actually does not have to know the exact phase function shape to achieve correct rendering results: in such scenarios, assuming a simple Henyey-Greenstein phase function with any fixed parameter g is sufficient, with the other parameters being scaled accordingly. Zhao et al. [2014] apply this principle to speed up Monte Carlo rendering of optically dense materials by recalculating their parameters to lower material densities with identical appearance.

On the flip side of the coin, the similarity theorem also means that *measuring* the phase function is a decidedly non-trivial problem: one has to identify the one correct parameter triplet (σ_a, σ_s, g) out of the potentially infinitely many possible solutions under the given measurement geometry.

Breaking similarity. The key to “breaking out of” the similarity relations to allow measuring the phase function seems to be using a

combination of measurement geometries that together disambiguate between the forward and backward scattering in the material. One example being our method, where we illuminate the measured sample from the front using diffuse illuminants, and from the back using a collimated beam. Other methods rely on shining a collimated beam through the sample and observing it from various angles. Such angular (gonio-photometric) measurements were presented for example by Gkioulekas et al. [2013] and Leyre et al. [2014].

3 LIST OF COMPONENTS

The following table provides a list of components that we used to build a prototype of our measurement method. Description of the method itself and its diagrams are provided in the main article.

Order code	Material sample
Thorlabs OILCL30 <i>local supplier</i>	Immersion oil, Cargille Type LDF, $n = 1.518$ Microscope glass slides, 24x50 mm, borosilicate glass 3.3, 0.14-0.17 mm
Diffuse backgrounds	
Thorlabs BFP1	Black Flocked Self-Adhesive Paper, 1% reflectance
Thorlabs BKF12	(alternative) Black aluminum foil, 5% reflectance
Ocean Insight WS-1-SL	Spectralon Diffuse Reflectance Standard, 99% reflectance, ~1in diameter
Thorlabs PMR10P1	(alternative) PTFE Diffuse Reflector Sheet, 92% reflectance
Detector	
Ocean Insight USB-650UV	Spectrometer
Ocean Insight P400-1-SR	Spectrometer fiber, 400 μm
Thorlabs SM05SMA	SMA Fiber Adapter Plate with External SM05 (0.535"-40) Threads
Flir LENS-250T5C	Tamron 25mm fixed local length C-mount lens (focusing light into the fiber)
Thorlabs CMR/M	C-Mount Camera Lens Mount, Post Mountable, M4 Tap (holds the lens)
Diffuse illumination	
Bellanny 100W	2x Warm white LED floodlight panel, 100 W
Collimated illumination	
OptoSupply OSM57L5201P	Warm white 5mm THT LED, 70 mA, 8° angle
OWON P4305	Low-voltage lab power supply
Thorlabs DG10-220	Ø1" Unmounted N-BK7 Ground Glass Diffuser, 220 Grit
Thorlabs LA1074	D=12.7 F=20.0 N-BK7 Plano Convex Lens (lens next to the LED)
Thorlabs LMR05/M	Lens Mount with Retaining Ring for Ø1/2" Optics, M4 Tap
Thorlabs DT12/M	12.7 mm Dovetail Translation Stage, M4 Taps ("mini-rail adjustable with a thumb screw" holding the small lens)
Thorlabs LEDMF	Ø1/2" Post-Mountable LED Mount for TO-18, TO-18R, and T-1 3/4 LEDs (LED holder)
Other optomechanical components	
N/A	1x 3D-printed background holder (rail and a holder)
Thorlabs P1000D	2x Ø1" Mounted Pinhole, 1000 μm , Stainless Steel
Thorlabs ID12/M	1x Mounted Standard Iris, Ø12 mm Max Aperture, TR75/M Post (adjustable pinhole before the background holder)
Thorlabs PH100/M-P5	10x Ø12.7 mm Post Holder, Spring-Loaded Hex-Locking Thumbscrew, L=100 mm (round, black): 3x for LED, diffuser+pinhole and lens, 1x for the "output" pinhole, 2+1x for the background+sample holder, 1x for the pinhole, 2x for the final lens + fiber
Thorlabs LMR1/M	3x Lens Mount with Retaining Ring for Ø1" Optics, M4 Tap (1x holds the LED mount, 1x holder for the diffuser+pinhole and 1x for the second non-adjustable pinhole)
Thorlabs TR100/M	13x Ø12.7 mm Optical Post, SS, M4 Setscrew, M6 Tap, L = 100 mm (silver post: 3x in the LED holder - connected with clamps, 10x in post holders)
Thorlabs BA1S/M	3x Mounting Base, 25 mm x 58 mm x 10 mm (2x in the diffuser/pinhole+lens holders, 1x for the adjustable pinhole holder)
Thorlabs UPH100/M	2x Ø12.7 mm Universal Post Holder, Spring-Loaded Locking Thumbscrew, L = 100 mm (1x bottom of the LED holder and 1x fiber holder)
Thorlabs RA90/M	3x Right-Angle Clamp for Ø1/2" Posts, 5 mm Hex (2x clamps in the LED holder, 1x holding the fiber)
Thorlabs FP01	1x Plate Holder, 0.9" Wide, Holds Plates up to 0.58" Thick (holds the measured samples)

REFERENCES

- Ioannis Gkioulekas, Shuang Zhao, Kavita Bala, Todd Zickler, and Anat Levin. 2013. Inverse Volume Rendering with Material Dictionaries. *ACM Trans. Graph.* 32, 6 (Nov. 2013), 162:1–162:13. <https://doi.org/10.1145/2508363.2508377>
- Wenzel Jakob and Johannes Hanika. 2019. A Low-Dimensional Function Space for Efficient Spectral Upsampling. *Computer Graphics Forum (Proceedings of Eurographics)* 38, 2 (March 2019).
- Johannes Jendersie. 2021. Fast Spectral Upsampling of Volume Attenuation Coefficients. In *Ray Tracing Gems II: Next Generation Real-Time Rendering with DXR, Vulkan, and OptiX*, Adam Marrs, Peter Shirley, and Ingo Wald (Eds.). Apress, Berkeley, CA, 153–159. https://doi.org/10.1007/978-1-4842-7185-8_13
- Alisa Jung, Alexander Wilkie, Johannes Hanika, Wenzel Jakob, and Carsten Dachsbacher. 2019. Wide Gamut Spectral Upsampling with Fluorescence. *Computer Graphics Forum (Proceedings of Eurographics Symposium on Rendering)* 38, 4 (Oct. 2019). <https://doi.org/10.1111/cgf.13773>
- Sven Leyre, Youri Meuret, Guy Durinck, Johan Hofkens, Geert Deconinck, and Peter Hanselaer. 2014. Estimation of the effective phase function of bulk diffusing materials with the inverse adding-doubling method. *Applied Optics* 53, 10 (April 2014), 2117. <https://doi.org/10.1364/AO.53.002117>
- Douglas R Wyman, Michael S Patterson, and Brian C Wilson. 1989. Similarity relations for anisotropic scattering in Monte Carlo simulations of deeply penetrating neutral particles. *J. Comput. Phys.* 81, 1 (March 1989), 137–150. [https://doi.org/10.1016/0021-9991\(89\)90067-3](https://doi.org/10.1016/0021-9991(89)90067-3)
- G. Wyszecki and W. S. Stiles. 1982. *Color Science: Concepts and Methods, Quantitative Data and Formulae*. Wiley.
- Shuang Zhao, Ravi Ramamoorthi, and Kavita Bala. 2014. High-order similarity relations in radiative transfer. *ACM Transactions on Graphics* 33, 4 (July 2014), 104:1–104:12. <https://doi.org/10.1145/2601097.2601104>